Applied Catalysis B: Environmental 168-169 (2015) 515–523

Contents lists available at ScienceDirect

Applied Catalysis B: Environmental

journal homepage: www.elsevier.com/locate/apcatb

Inorganic hydroxide fluorides as solid catalysts for acylation of 2-methylfuran by acetic anhydride

Fatima Frouri, Stéphane Célérier*, Philippe Ayrault, Frédéric Richard

Institut de Chimie des Milieux et Matériaux de Poitiers (IC2MP), UMR CNRS 7285, Faculté des Sciences Fondamentales et Appliquées, Université de Poitiers, 4, rue Michel Brunet, Bat B27, TSA 51106, 86073 Poitiers Cedex 9, France

ARTICLE INFO

Article history:
Received 27 November 2014
Received in revised form 13 January 2015
Accepted 17 January 2015
Available online 20 January 2015

Keywords:
Aluminum hydroxide fluoride
Bi-acidic solid catalyst
Acylation
2-Methylfuran
2-Acetyl-5-methylfuran

ABSTRACT

Several inorganic hydroxide fluorides $MF_{n-x}(OH)_x$ with *M* being either aluminum, iron, or magnesium were synthesized using a sol–gel method. These mesoporous fluoride materials exhibited very high specific surface areas (between 60 and 370 $m^2\,g^{-1}$) depending on the synthesis parameters used (nature of the metal, HF/Al ratio, and thermal treatment). It is shown that their acidic properties can also be adjusted by tuning these parameters. Indeed, in the case of aluminum hydroxide fluorides, bi-acidic catalysts containing both Brønsted and Lewis acid sites were obtained, the amount of acid sites and the Lewis/Bronsted ratio (in the range of 1.9–7.6) being very dependent on the synthesis parameters. For example, the increase of the calcination temperature of aluminum hydroxide fluorides led to a decrease of both Lewis and Brønsted acid site, but also an increase of the Lewis/Bronsted ratio. The most acid fluoride exhibited 542 $\mu mol\,g^{-1}$ of Lewis acid sites and 291 $\mu mol\,g^{-1}$ of Brønsted acid sites.

These inorganic hydroxide fluorides were successively used as catalysts for the solvent-free acylation of 2-methylfuran by acetic anhydride under mild conditions (50 °C, atmospheric pressure) yielding selectively 2-acetyl-5-methylfuran. The activity of fluoride can be related to the amount of both Lewis and Brønsted acid sites. In general the higher these values, the greater the activity in acylation. A reaction mechanism was proposed involving a bi-acidic site which could be a Lewis acid site (unsaturated aluminum) in the vicinity of a Brønsted acid site.

1. Introduction

Today, the investigation of new and alternative methodologies for the production of chemicals using low environmental impact technologies than those currently available is a major challenge for the scientific community. In this way, lignocellulosic residues can constitute a highly promising raw materials for the production of chemicals. For example, furfural can be produced by hydrolysis and dehydration of xylan which is a polysaccharide contained in hemicellulose [1]. This compound is considered as a promising platform molecule, since it can be used for the synthesis of several non-petroleum derived chemicals and fuels [2–5]. For example, furfural can be selectively hydrogenated into 2-methylfuran over metallic catalysts [6]. Its valorization into higher-value added products could be performed through Friedel–Crafts acylation reaction, since ketone functional group containing heterocyclic aromatic compounds are known to be valuable intermediates of pharmaceutical chemistry [7].

Traditionally, the Friedel–Crafts synthesis is carried out in liquid-phase by using either protonic (HF, H_2SO_4) or Lewis acids ($AlCl_3$, $FeCl_3$, and $TiCl_4$) as catalysts [8]. Nevertheless, the commonly encountered drawbacks of such a synthesis include the difficulty of catalysts separation and problems of waste disposal.

In the line with more stringent environmental legislation from the last years, the search for highly efficient and cleaner processes often leads to the replacement of homogeneous catalysts by heterogeneous catalysts [9]. Indeed, the use of solid catalysts offers definite advantages compared to homogeneous catalysts, since the former are easy to recover by simple filtration and produce no salts. In this way, the development of new and increasingly efficient solid catalysts for Friedel–Crafts acylation can be considered as a challenging task, particularly to address problems mentioned above.

Several acidic zeolites, like HZSM-5, HY, and Hβ were often used as catalysts for the acylation of oxygenated heterocyclic compounds, such as furan [10,11] and benzofuran [12–14]. For example, the acylation of furan by acetic anhydride in vapour phase (150 °C,

* Corresponding author. Tel.: + 33 549 453 674; fax: +33 549 453 899.
E-mail address: stephane.celerier@univ-poitiers.fr (S. Célérier).

http://dx.doi.org/10.1016/j.apcatb.2015.01.020

atmospheric pressure) over both HZSM-5 and HY zeolites led selectively to 2-acetylfuran with yields of 37 mol% and 21.6 mol%, respectively [11]. Over Hβ zeolite, under milder experimental conditions (liquid phase, 60 °C, atmospheric pressure), in presence of a large excess of acetic anhydride (ratio furan to acylating agent of 5), 2-acetylfuran was also selectively synthesized with a yield of 91 mol% after 120 min [10]. Nevertheless, zeolites are known to be very sensitive to deactivation, especially when they were used as catalysts for acylation [14–17]. For example, the strong deactivation of the Hβ zeolite observed during the acylation of anisole with acetic anhydride was mainly attributed to a strong adsorption of the mono-acylated product (*p*-methoxyacetophenone) on the acid sites [15]. A pore blocking by polyacylated products would also explain a part of the zeolite deactivation [15,16].

In the past decade, metal fluorides, such as MgF_2 and AlF_3, with significant surface areas were successfully used in different heterogeneous catalytic processes with promising results as catalysts [18–23] and supports [24–27]. Specifically, in 2003, Kemnitz et al. have developed a sol–gel synthesis leading to the formation of amorphous aluminum fluoride with very high specific surface area and very high Lewis acidity [28]. From this first work, this group declined this synthesis method to the development of several nanoscopic metal fluorides or hydroxide fluorides $MF_{n-x}(OH)_x$ with different acid–base properties [29–33]. Thus, by altering the synthesis parameters (fluoride – metal ratio, nature of metal, and amount of water during the synthesis), the authors showed that the strength and the nature of acid and basic properties (Brønsted and Lewis) might be adjustable.

Bi-acidic fluorine containing solids prepared by sol–gel method have been used recently as catalysts for Friedel–Crafts alkylation allowing the synthesis of two vitamins (K_1 and K_1-Chromanol) in high yields (between 58 and 71 mol%) [34]. The alkylation of various aromatic compounds (benzene, ethylbenzene, trimethylhydroquinone, and menadiol) with isophytol and benzyl alcohol under mild conditions (100–120 °C) was also investigated over MgF_2 and AlF_3 catalysts [35]. Both solids were found as efficient catalysts for the synthesis of diphenylmethane and *p*-ethyldiphenylmethane. In the same way, menadiol was selectively acylated by an excess of acetic anhydride into menadiol diacetate at 80 °C over AlF_3 and MgF_2 [36].

As the development of clean catalytic processes is an important topic of environmental protection, we propose to develop the use of metal hydroxide fluorides $MF_{n-x}(OH)_x$ (M = Al, Mg, and Fe) as bi-acidic solid catalysts for the synthesis of 2-acetyl-5-methylfuran. For this purpose, the acylation of 2-methylfuran by acetic anhydride was carried out under mild experimental conditions (50 °C, atmospheric pressure) over these catalysts. Their acidic properties were adjusted by modifications of some parameters of the catalyst synthesis: nature of the metal, Fluorine/Metal ratio, and thermal treatment. Based on their extensive characterization (obtained by nitrogen adsorption, XRD, TEM, and adsorption of pyridine followed by FTIR) and their catalytic properties measured in Friedel–Crafts acylation, some proposals concerning active sites involved and reaction mechanism were discussed.

2. Experimental

2.1. $MF_{n-x}(OH)_x$ hydroxide fluorides synthesis (M = Al, Mg, Fe)

Caution: HF is hazardous; protection required.

$AlF_{3-x}(OH)_x$ powders were prepared by sol–gel method, partly based on the work of Coman et al. [37]. In a first step, 4.9 g of aluminum isopropoxide (Aldrich, ≥98%) were introduced in 150 mL of methanol (Sigma–Aldrich, ≥99.9%) and after stirring during 20 min, stoichiometric amount of aqueous HF (3.02 g, 48–wt% HF in water, Sigma–Aldrich, 99.99%) was added to this suspension under stirring conditions. After addition of HF, this solution was stirred during 8 h and aged at ambient temperature for one night. Then, the obtained sol was dried in an oven at 100 °C for 24 h to obtain a white powder, named AlF_3-100 (where the number corresponds to the drying temperature). The AlF_3-100 sample was then calcined under dry air at different temperatures between 150 and 350 °C during 5 h and the obtained powders were called AlF_3-xxx where xxx corresponds to the temperature of calcination.

In some specific experiments, sub-stoichiometric amount of aqueous HF was introduced to obtain two different HF/Al ratios: 2.9 and 2.5. These powders were then calcined under dry air at 150 °C during 5 h and named $AlF_{2.9}$-150 (from the HF/Al ratio of 2.9) and $AlF_{2.5}$-150 (from the HF/Al ratio of 2.5).

The synthesis of $MgF_{2-x}(OH)_x$ powder by a sol–gel method was based on the work of Wuttke et al. [38]. In a first step, magnesium metal (1.56 g, Aldrich, 99.98%) was treated with an excess of anhydrous methanol (50 mL, Sigma–Aldrich, ≥99.8%) under reflux conditions for 6 h to form $Mg(OCH_3)_2$ metal alkoxide solution. Then, stoichiometric amount of aqueous HF (5.3504 g, 48 wt% HF in water) was added to this solution under stirring conditions. A highly exothermic reaction was performed to obtain a sol (gel was not formed due to the stirring conditions). This sol was stirred for 24 h, aged at ambient temperature for 24 h and dried at 100 °C for 24 h to form the powder named MgF_2-100.

The synthesis of $FeF_{3-x}(OH)_x$ powder by sol–gel method is based on the work of Guo et al. [30]. In a first step, $Fe(NO_3)_3{\cdot}9H_2O$ (11.7 g, Sigma–Aldrich, ≥98%) was pre-treated under vaccum at 65 °C during 2 h to form $Fe(OH)(NO_3)_3{\cdot}2.2H_2O$. This powder was dissolved in 150 mL of anhydrous methanol (Sigma–Aldrich, ≥99.8%) and after stirring, 9.65 g of anhydrous methalonic HF solution (18 wt% HF in anhydrous methanol) were added to form a transparent sol. After stirring during 1 h, the sol was dried under vaccum at 70 °C to form a powder. This powder was calcined under dry air at 100 °C during 5 h and named FeF_3-100.

2.2. Zeolite

The commercial HY zeolite (CBV740) was provided by Conteka. This solid was activated at 450 °C under dry air for 6 h before catalytic experiments.

2.3. Catalyst characterization

XRD analysis of material powders was carried out on a PANalytical EMPYREAN powder diffractometer using CuKα radiation source ($K\alpha_1$ = 1.5406 Å and $K\alpha_2$ = 1.5444 Å) in order to reveal the crystallographic structure of each sample. These patterns were collected with a 0.02° step and 120 s dwell time at each step between 15 and 70°. Phase identification was performed by comparison with the JCPDS database reference files.

Nitrogen adsorption–desorption was performed at −196 °C using a TRISTAR 3000 gas adsorption system. Prior N_2 adsorption, the powder samples were degassed under secondary vacuum for 12 h at 70 °C. The BET equation was used to calculate the surface area (S_{BET} in $m^2\,g^{-1}$) of the samples at relative pressures between 0.05 and 0.30.

The average pore size (d_p in nm) was obtained from the desorption branch of the N_2 adsorption–desorption isotherm using Barret–Joyner–Halenda (BJH) approach.

The morphology of $AlF_{3-x}(OH)_x$ powders was evaluated by Transmission Electronic Microscopy (TEM), using a JEOL 2100 instrument (operated at 200 kV with a LaB_6 source and equipped with a Gatan Ultra scan camera).

The acidity of solid materials was measured by adsorption–desorption of pyridine followed by FTIR spectroscopy

Table 1
Microstructural and acidic properties of HY zeolite and hydroxide fluoride catalysts.

Entry	Catalyst	S_{BET}[a] ($m^2\,g^{-1}$)	Average pores size d_p[b] (nm)	Acidity Brønsted ($\mu mol\,g^{-1}$)[c]	Lewis ($\mu mol\,g^{-1}$)[d]	Ratio L/B[e]
1	AlF_3-100	370	3.4	291	542	1.9
2	AlF_3-150	239	4.4	192	397	2.1
3	AlF_3-200	151	5.6	135	381	2.8
4	AlF_3-350	97	8.6	61	246	4.0
5	$AlF_{2.9}$-150	252	6.9	159	464	2.9
6	$AlF_{2.5}$-150	179	7.1	54	419	7.6
7	MgF_2-100	332	4.6	7	387	55.3
8	FeF_3-100	61	10.0	0	145	–
9	HY	632	0.7[f]	214	84	0.4

[a] Specific surface area calculated by the BET method.
[b] Determined with the BJH approach.
[c] Deduced from the intensity of the band located around 1540–1550 cm^{-1} obtained from the adsorption–desorption of pyridine followed by IR.
[d] Deduced from the intensity of the band located around 1454 cm^{-1} obtained from the adsorption–desorption of pyridine followed by IR.
[e] L = amount of Lewis acid sites, B = amount of Brønsted acid sites.
[f] From [41].

using a ThermoNicolet NEXUS 5700 spectrometer with a resolution of 2 cm^{-1} and 128 scans per spectrum. Material samples were pressed into thin pellets (10–30 mg) with diameter of 16 mm under a pressure of 1–2 t cm^{-2} and activated *in situ* during one night under vacuum (10^{-5} Pa) at 150 °C. Pyridine was introduced in excess at 150 °C after the activation period. The solid sample was vacuum-packed to eliminate physisorbed pyridine and IR spectrum was recorded at 150 °C. The concentrations of the Brønsted and Lewis sites were determined from the integrated area bands of the PyH^+ (located between 1540 and 1550 cm^{-1}) and PyL (located between 1445 and 1455 cm^{-1}) species using the values of the molar extinction coefficients of both bands (1.13 and 1.28 cm μmol^{-1}, respectively) [39].

2.4. Catalytic tests

The reaction was carried out in a batch reactor fitted with a magnet stirrer and heated in a synthetic oil bath at 50 °C. The catalyst (500 mg) was introduced in a mixture composed by 2-methylfuran (61 mmol, Sigma–Aldrich, 99%), acetic anhydride (66 mmol or 133 mmol, Sigma–Aldrich, >99%) and nonane (4 mmol, Sigma–Aldrich, 99%), the latter compound was used as an internal standard for quantitative analysis by Gas Chromatography. The progress of the reaction was monitored by using a Varian 430 chromatograph equipped with CPSIL–5CB capillary column (length: 50 m; diameter: 0.25 mm, and film thickness: 5 μm) and a flame ionization detector. The oven temperature was programmed from 50 °C (maintained during 1 min) to 250 °C (5 °C/min). The only product obtained, 2-acetyl-5-methylfuran, was identified by co-injection of the commercial compound (Sigma–Aldrich, 98%) and by using Varian 3800 chromatograph coupled with a 1200 TQ mass spectrometer.

3. Results and discussion

3.1. Influence of the calcination temperature of aluminum hydroxide fluorides ($AlF_{3-x}(OH)_x$) as catalysts for acylation of 2-methylfuran by acetic anhydride

As indicated in the experimental part, the powder named AlF_3-100 was obtained by sol–gel synthesis after drying at 100 °C. In this process, a metal alkoxide was reacted with stoichiometric amount of aqueous HF. Briefly, a competition between fluorolysis (reaction with HF) and hydrolysis (reaction with water) occurred resulting in the formation of $AlF_{3-x}(OH)_x$ hydroxide fluorides, in favor of the former. Kinetically, the fluorolysis rate is higher than the hydrolysis rate leading to the dominant formation of the metal fluoride

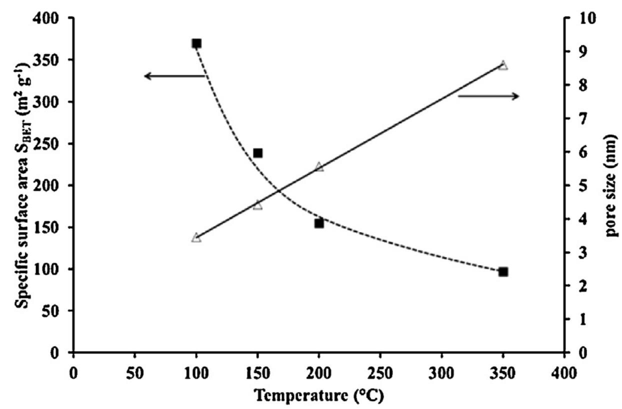

Fig. 1. Influence on the calcination temperature of aluminum hydroxide fluorides ($AlF_{3-x}(OH)_x$) on their specific surface areas (■) and their pore sizes (△).

[35,40]. However, the presence of water in the media allowed the formation of a small amount of hydroxyl group ($x < 0.1$) on the $AlF_{3-x}(OH)_x$ metal hydroxide fluorides. As x is quite low, its value could not be determined by using conventional titration methods. However, the presence of such groups has already been evidenced on this kind of materials prepared by the same method [37]. This is summarized by the following equations:

$$Al(OR)_3 + 3HF \rightarrow AlF_3 + 3ROH \text{ fluorolysis reaction,}$$

$$Al(OR)_3 + 3H_2O \rightarrow Al(OH)_3 + 3ROH \text{ hydrolysis reaction}$$

In aqueous HF with stoichiometric amount of HF:

$$Al(OR)_3 + 3HF + xH_2O \rightarrow AlF_{3-x}(OH)_x + 3ROH + xHF \text{ (with } x < 0.1).$$

The powder named AlF_3-100 was calcined under dry air at different temperatures between 150 and 350 °C to produce different catalysts. All synthesized hydroxide fluorides were amorphous even after calcination at 350 °C. However, after calcination under dry air at higher temperature (900 °C), the formation of AlF_3 with the rhombohedral structure was observed by XRD without formation of oxide phase confirming the final formation of an aluminum fluoride by this synthesis method (XRD pattern not shown here). Their amorphous character was consistent with the formation of nanoscopic material with very high specific surface area. Indeed, after drying at 100 °C, the specific surface area of AlF_3-100 was 370 $m^2\,g^{-1}$ (Table 1, entry 1). As expected, an increase of the calcination temperature of fluorides led to a decrease of their specific surface area (Fig. 1). Nevertheless, the specific surface area

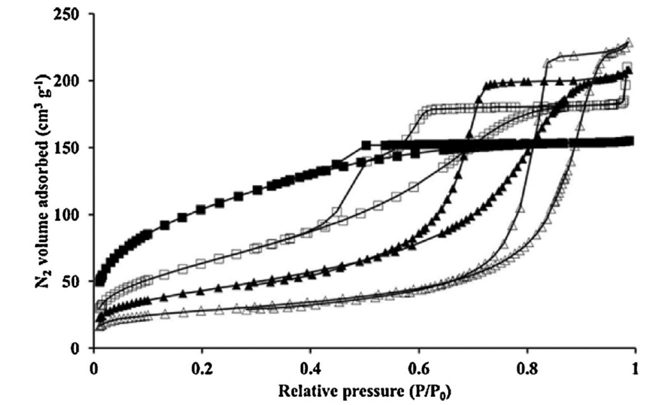

Fig. 2. Nitrogen adsorption–desorption isotherms of aluminum hydroxide fluorides: AlF_3-100 (■), AlF_3-150 (□), AlF_3-200 (▲) and AlF_3-350 (△).

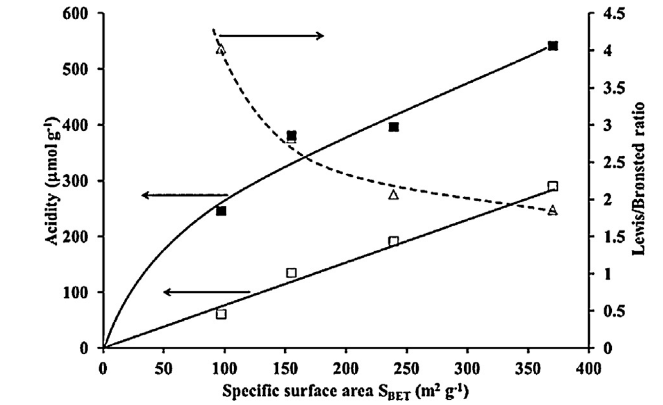

Fig. 4. Concentration of Brønsted (□) and Lewis (■) acid sites determined by adsorption–desorption of pyridine followed by IR and Lewis/Brønsted ratio (△) as a function of the specific surface area of the aluminum hydroxide fluoride ($AlF_{3-x}(OH)_x$) samples.

remained relatively high, equal to 97 $m^2 g^{-1}$, even when calcined at 350 °C (Table 1, entry 4).

The adsorption–desorption isotherms of all solid samples are shown in Fig. 2. A type IV isotherm according to the IUPAC classification was observed for all solids whatever the calcination temperature used, indicating the preservation of the mesoporous network of the aluminum hydroxide fluoride. In addition, the increase of the calcination temperature led to a shift of the hysteresis curve to the higher relative pressure P/P_0 due to an increase in pore size. This is confirmed by the value of the average pore size of each sample determined by the BJH method (Table 1). For example, the average pore size value of the AlF_3-100 sample was 3.4 nm and this size increased linearly until 8.6 nm for the sample calcined at 350 °C, as shown in Fig. 1.

Two aluminum hydroxide fluorides were characterized by TEM analysis: the AlF_3-100 sample exhibited small particles, with diameters between 6 and 10 nm, whereas, the AlF_3-350 sample showed particles with a diameter between 20 and 40 nm (Fig. 3).

To summarize, the thermal treatment under dry air led to aggregation and/or sintering phenomena (increase of particle size) of the aluminum hydroxide fluorides ($AlF_{3-x}(OH)_x$) resulting in a decrease of the specific surface area along with an increase of pore size.

As reported in Table 1, these aluminum hydroxide fluorides have Brønsted and Lewis acid sites, which quantities were estimated based on adsorption–desorption of pyridine followed by IR. As discussed above in this part, the sol–gel synthesis of $AlF_{3-x}(OH)_x$ with aqueous HF led to the formation of a small amount of hydroxyl groups, which were Brønsted acid sites as proposed in the literature [37]. Moreover, many under-coordinated metals were present at the surface of these materials, corresponding to Lewis acid sites. Thus, bi-acidic catalysts (Lewis and Brønsted) could be prepared by this method.

The modification of the microstructure of aluminum hydroxide fluoride samples with the temperature of calcination led also to a modification of the acidic properties, as depicted in Fig. 4. Indeed, the increase of the specific surface areas of such solids, obtained by the reduction of the calcination temperature, led to an increase of both Brønsted and Lewis acid sites, the AlF_3-100 sample showing the highest amount of Brønsted (291 µmol g^{-1}) and Lewis (541 µmol g^{-1}) acid sites (Table 1, entry 1).

While the Lewis acid sites were always in the majority in these aluminum hydroxide fluorides, it was also worth noting that the Lewis/Brønsted ratio, in the range of 1.9–4.0, could be tuned with the temperature of calcination and hence the specific surface area. This phenomenon could be explained by the dehydration of the material with the thermal treatment leading to a gradual elimination of hydroxyl group of the material affecting their Brønsted acidity whereas, the amount of Lewis acid sites was less affected. It may be noted that Coman et al. [34,37] also demonstrated previously the possibility to modify the ratio of Lewis/Brønsted sites by the amount of water introduced during the sol–gel synthesis of $AlF_{3-x}(OH)_x$.

The acylation of 2-methylfuran by acetic anhydride (Scheme 1) was carried out in the presence of these bi-acidic (Brønsted and Lewis) solid catalysts. Over all catalysts, this reaction produced

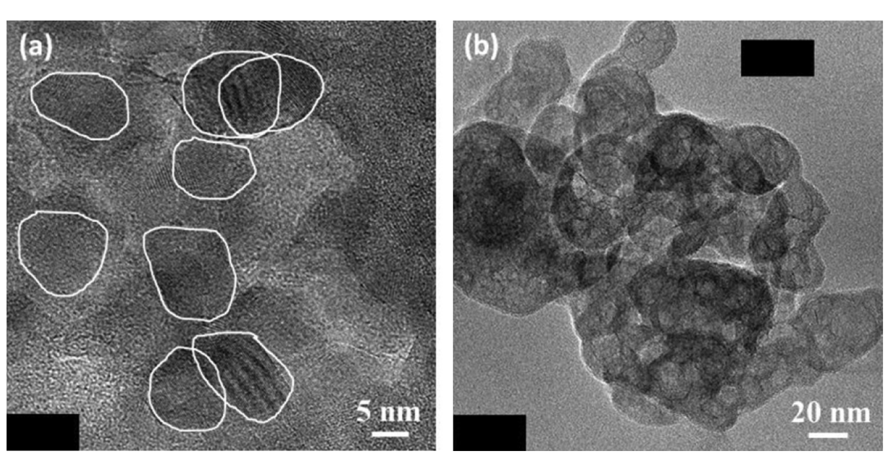

Fig. 3. TEM images obtained for AlF_3-100 (a) and AlF_3-350 (b). For the AlF_3-100 sample, some particles are surrounded for sake of clarity.

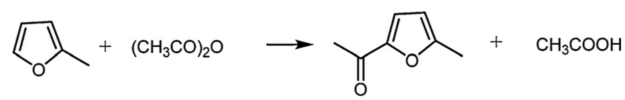

Scheme 1. Acylation of 2-methylfuran by acetic anhydride leading to 2-acetyl-5-methylfuran and acetic acid.

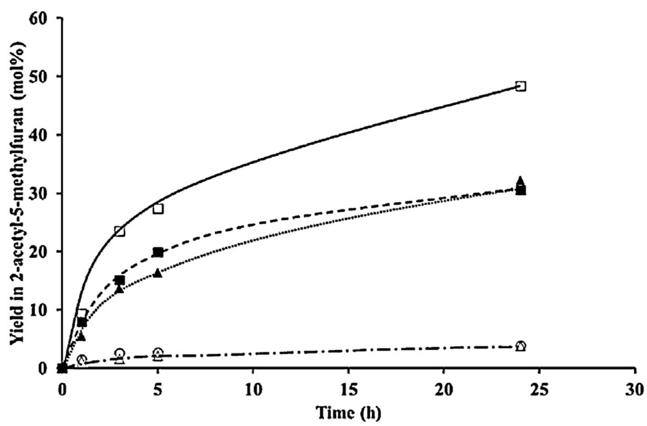

Fig. 5. Acylation of 2-methylfuran (61 mmol) by acetic anhydride (67 mmol) at 50 °C over HY zeolite (○) and aluminum hydroxide fluoride catalysts ($w_{catalyst}$ = 500 mg): AlF_3-100 (■), AlF_3-150 (□), AlF_3-200 (▲) and AlF_3-350 (△).

selectively 2-acetyl-5-methylfuran. Fig. 5 shows that the yield in 2-acetyl-5-methylfuran as a function of time depended on the aluminum hydroxide fluoride catalyst used. The aluminum fluoride solid calcined at 150 °C (AlF_3-150) was the most active catalyst for the acylation of 2-methylfuran by acetic anhydride. Indeed, a yield of 48 mol% was obtained after 24 h of reaction with this catalyst whereas 32, 30, and 4 mol% were obtained with AlF_3-200, AlF_3-100, and AlF_3-350, respectively. As it can be seen on Fig. 6, a correlation between the performances and the acidic properties (both Lewis and Brønsted acidities) of the fluorides calcined in the range of 150–350 °C can be highlighted. Indeed, the yield in 2-acetyl-5-methylfuran increased linearly with the amount of Lewis and Brønsted acid sites present in these materials. Assuming the possibility that the two acid sites can play a role in the reaction mechanism of acylation involving a bi-acid catalytic site, its nature being discussed in the 3.5 part of this paper, the amount of Brønsted acid sites could be the limiting parameter. Indeed, there are fewer Brønsted sites than Lewis sites on each catalyst, which could explain the better correlation between the yield in acylated product and the amount of Brønsted acid sites (Fig. 6).

Nevertheless, the activity of the AlF_3-100 sample, the most acidic aluminum fluoride synthesized in this study, was much lower than the expected value based on its acidic properties. The low activity of this catalyst could be explained by different reasons. Firstly, as shown previously, this solid presented the smallest pores (Table 1) leading to significant constraints concerning the diffusion of reactants to the active sites. Secondly, the great amount of acid sites on this catalyst could lead to its fast deactivation rate owing to a high amount of adsorbed acylated products. Nevertheless, under our experimental conditions (batch reactor), it was very difficult to measure precisely the deactivation rate of fluoride catalysts. Thirdly, the acidity of this sample was not determined at 100 °C, its calcination temperature, but at 150 °C in order to eliminate physisorbed pyridine, which could eliminate also adsorbed water. Therefore, it could be possible that water molecules remain adsorbed on acid sites of the AlF_3-100 sample partially inhibiting its catalytic activity.

3.2. Comparison between HY zeolite and $AlF_{3-x}(OH)_x$ as catalysts for acylation of 2-methylfuran by acetic anhydride

The catalytic performances of aluminum hydroxide fluorides were compared with data obtained from a commercial HY zeolite. As expected, the zeolitic material exhibited mainly Brønsted acidity (Table 1, entry 9), which was close to that of AlF_3-150, its L/B acidity ratio being equal to 0.4. As in the case of $AlF_{3-x}(OH)_x$, 2-acetyl-5-methylfuran was the only acylated product observed over HY from the reaction between 2-methylfuran and acetic anhydride. Nevertheless, this zeolite was much less active than AlF_3-150 and presented the same activity as AlF_3-350 (Fig. 5), showing that aluminum hydroxide fluoride material is a more efficient catalyst than the HY zeolite for Friedel–Crafts acylation, especially for acylation of 2-methylfuran by acetic anhydride. The low activity of HY in acylation of 2-methylfuran could be explained by the low amount of Lewis acid sites over HY in comparison with aluminum hydroxide fluoride material, since these sites are probably involved in the reaction mechanism as discussed part 3.5 of this paper. Nevertheless, another reason can not be discarded to explain the lowest yield of 2-acetyl-5-methylfuran formed over HY compared to AlF_3-150, this could be linked to a fast deactivation rate for zeolitic materials, as already proposed for this kind of reaction [15]. Indeed, a pore blocking by heavier compounds entrapped in the microporous zeolitic structure, which exhibited a low pore opening (7.4 Å) [41], could favor the deactivation process of zeolite. Consequently, it could be proposed that the active sites of fluoride materials may be less sensitive to deactivation than the acid sites of zeolitic materials.

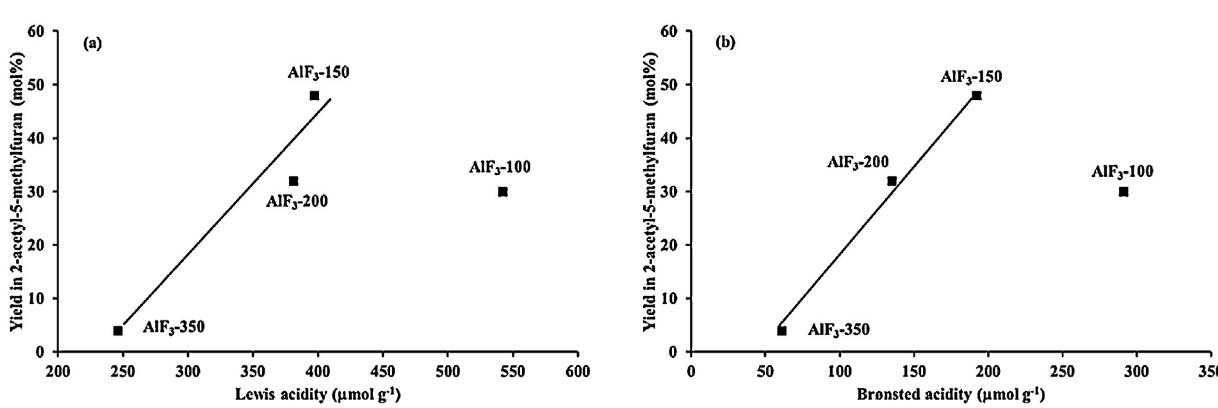

Fig. 6. Acylation of 2-methylfuran (61 mmol) by acetic anhydride (67 mmol) at 50 °C over aluminum hydroxide fluoride catalysts ($w_{catalys}$ = 500 mg). Effect of the Lewis acidity (a) and the Brønsted acidity (b) on the yield in 2-acetyl-5-methylfuran.

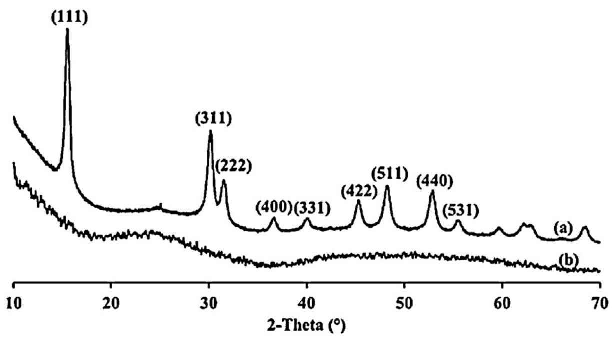

Fig. 7. X-ray diffraction patterns of $AlF_{2.5}$-150 (a) and $AlF_{2.9}$-150 (b). The main hkl indices of the pyrochlore aluminum hydroxyfluoride structure (Fd-3 m space group) are reported in brackets.

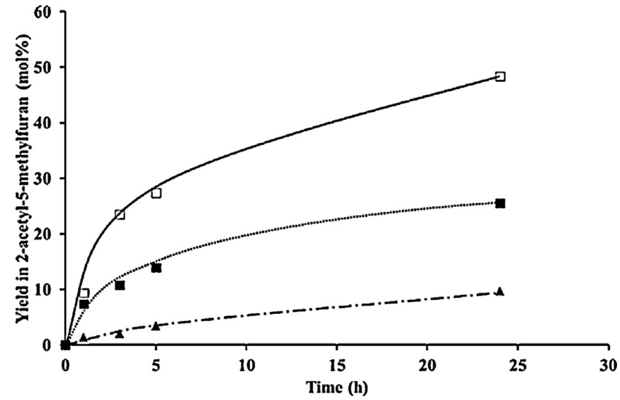

Fig. 8. Acylation of 2-methylfuran (61 mmol) by acetic anhydride (67 mmol) at 50 °C over aluminum hydroxide fluoride catalysts synthetized with different HF/Al ratio ($w_{catalys}$ = 500 mg): AlF_3-150 (□), $AlF_{2.9}$-150 (■) and $AlF_{2.5}$-150 (▲).

3.3. Influence of the HF/Al ratio during the sol–gel synthesis for acylation of 2-methylfuran by acetic anhydride

In order to tune the Lewis/Brønsted ratio of the aluminum hydroxide fluorides ($AlF_{3-x}(OH)_x$), the ratio between the amount of HF and the aluminum alkoxide was varied between 3 and 2.5. As reported by Kemnitz and co-workers [26,42], the synthesis of metal fluorides in sub-stoichiometry of HF by sol–gel method in presence of water led to the formation of $AlF_{3-x}(OH)_x$ with x corresponding approximately to the initial HF/Al ratio. Thus, by varying the HF/Al ratio from 3 to 2.5, the amount of hydroxyl groups is expected to increase. By this approach, several catalysts with different HF/Al ratio were prepared and calcined at 150 °C: AlF_3-150, $AlF_{2.9}$-150, and $AlF_{2.5}$-150. Both AlF_3-150 and $AlF_{2.9}$-150 were amorphous whereas, $AlF_{2.5}$-150 exhibited a cubic pyrochlore framework (Fd-3 m) as shown in Fig. 7, in accordance with results reported by Dambournet et al. [43]. This crystallized state could explain the lower specific surface area of this material (179 $m^2\,g^{-1}$) in comparison with both AlF_3-150 and $AlF_{2.9}$-150 which exhibited higher and similar specific surface areas, 239 and 252 $m^2\,g^{-1}$, respectively (Table 1).

The acidic properties of these solids were also characterized by adsorption–desorption of pyridine followed by IR spectroscopy (Table 1, entries 2, 5, and 6). While Lewis acidity was comparable between each catalyst (around 400 $\mu mol\,g^{-1}$), the Brønsted acidity clearly evolved. Indeed, the amount of Brønsted acid sites was 192 $\mu mol\,g^{-1}$ for AlF_3-150 and only 54 $\mu mol\,g^{-1}$ for $AlF_{2.5}$-150, the behavior of $AlF_{2.9}$-150 being intermediate (159 $\mu mol\,g^{-1}$). Thus, despite a larger amount of hydroxyl groups with the decrease of HF/Al ratio, the amount of Brønsted acid sites decreased. This result can be explained by the stronger inductive effect of fluorine (most electronegative element) in comparison with hydroxyl groups. Thus, the presence of higher amount of fluorine atoms in AlF_3-150 in comparison with $AlF_{2.5}$-150 could explain the higher amount of Brønsted acid sites measured over AlF_3-150. Therefore, it can be proposed that most of hydroxyl groups present in $AlF_{2.5}$-150 are probably not acid due to the lack of fluorine atom in their environment. The low amount of Brønsted acid sites on the $AlF_{2.5}$-150 exhibiting a pyrochlore structure is consistent with the literature [43]. As expected, the ratio Lewis/Brønsted could be tuned with the HF/Al ratio during the sol–gel synthesis from 2.1 (AlF_3-150) to 7.6 ($AlF_{2.5}$-150) as indicated in Table 1.

The modification of the acidic properties of such hydroxide fluorides led also to different behaviors concerning their activity in acylation reaction, as shown in Fig. 8. Indeed, after 24 h of reaction, the yield in 2-acetyl-5-methylfuran was the highest (close to 48 mol%) with the catalyst prepared with a HF/Al ratio of 3 (AlF_3-150) and the lowest (close to 10 mol%) with the catalyst prepared with a HF/Al ratio of 2.5 ($AlF_{2.5}$-150), probably due to the reduced amount of Brønsted acid sites. A correlation between the activity in acylation (measured by the yield in 2-acetyl-5-methylfuran obtained after 24 h) and the amount of Brønsted acid sites was highlighted (Fig. 9). Unfortunately, such a correlation was not observed concerning the Lewis acidity, which was likely due to a large excess of Lewis acid sites compared to Brønsted acid sites for the three catalysts. Nevertheless, it is obvious that the Brønsted acidity of aluminum hydroxyl fluorides plays an important role to explain their activity in acylation reaction.

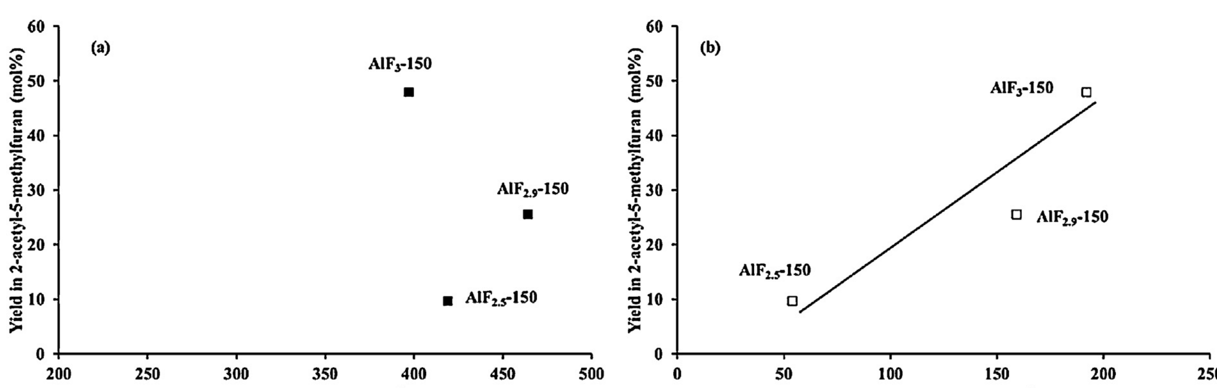

Fig. 9. Acylation of 2-methylfuran (61 mmol) by acetic anhydride (67 mmol) at 50 °C over aluminum hydroxide fluoride catalysts synthetized with different HF/Al ratio ($w_{catalyst}$ = 500 mg). Effect of the Lewis acidity (a) and the Brønsted acidity (b) on the yield in 2-acetyl-5-methylfuran.

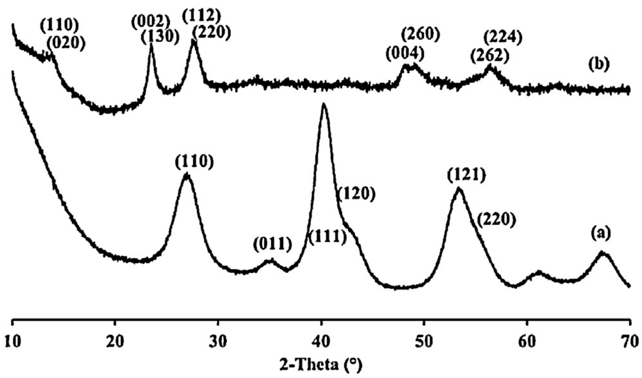

Fig. 10. X-ray diffraction patterns of MgF_2-100 (a) and FeF_3-100 (b). The main hkl indices of the magnesium fluoride structure (P42/m nm, tetragonal) and of the iron fluoride hydrate (Cm cm, orthorhombic) are reported in brackets.

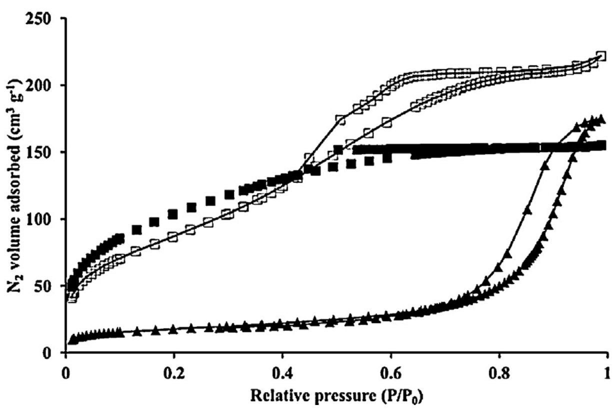

Fig. 11. Nitrogen adsorption–desorption isotherms of AlF_3-100 (■), MgF_2-100 (□), and FeF_3-100 (▲).

3.4. *Influence of the nature of metallic ion into hydroxide fluorides ($MF_{n-x}(OH)_x$)*

Another possibility to modify the acidity of fluoride solids is to replace aluminum by other metallic ions. For example, Kemnitz and co-workers have shown previously the possibility to obtain bi-acidic catalyst with iron fluoride [30] and magnesium fluoride [18] by sol–gel synthesis. For iron fluoride, a pre-treatment at 65 °C of the iron nitrate precursor was necessary to introduce Brønsted acid sites. For magnesium fluoride, as in the case of aluminum fluoride, the use of aqueous HF with metal alcoxyde led to introduce Brønsted acid sites. As indicated in the experimental part, both fluorides were calcined at 100 °C.

X-ray diffraction patterns of MgF_2-100 and FeF_3-100 show that both solids were crystallized (Fig. 10). The structure of MgF_2-100 was tetragonal (P42/m nm), and that of FeF_3-100 was orthorhombic (Cm cm) corresponding to FeF_3, 0.33H_2O. Their specific surface areas reported in Table 1 (entries 7 and 8) were compared with that of AlF_3-100 (Table 1, entry 1). The AlF_3-100 sample exhibited the highest specific surface area (370 $m^2\,g^{-1}$) and FeF_3-100 the lowest (61 $m^2\,g^{-1}$). The relatively low surface area of the FeF_3-100 sample was already reported by Guo et al. [30]. Fig. 11 shows that a type IV isotherm according to the IUPAC classification was observed for each sample indicating a mesoporous network whatever the fluoride synthesized. Nevertheless, the three solids clearly exhibited pores with different sizes as reported in Table 1.

The characterization of the acidic properties of both iron and magnesium fluoride samples, determined by adsorption–desorption of pyridine at 150 °C followed by IR spectroscopy, is reported in Table 1 (entries 7 and 8). In these conditions of characterization, both fluorides (MgF_2-100 and FeF_3-100) did not exhibit strong Brønsted acid sites, namely sites able to retain adsorbed pyridine at least at 150 °C. Although Brønsted sites have been observed on these materials [19,30], we did not observe it in the present work, probably due to the weakness of the acid sites.

The amount of Lewis acid sites was also lower on these both fluoride samples compared to aluminum hydroxide fluoride (AlF_3-100), the FeF_3-100 sample containing the lowest amount of these sites (145 $\mu mol\,g^{-1}$) as reported in Table 1. Moreover, according to the shift of the band characteristic of pyridine adsorbed on Lewis acid sites located between 1610 and 1625 cm^{-1} (spectra not shown here), it seems that the strength of Lewis acidity depended on the fluoride solid according to the following scale: AlF_3-100 (1623 cm^{-1}) > FeF_3-100 (1613 cm^{-1}) > MgF_2-100 (1609 cm^{-1}). Indeed, it is well known that the higher the band shift, the higher the strength [44]. Consequently, these results clearly indicates that a benefit of using several inorganic fluorides is the possibility to tune the strength of Lewis acidity with the chemical nature of the metal, as already reported in the literature [23,29].

Both FeF_3-100 and MgF_2-100 fluorides were evaluated as catalysts for the acylation of 2-methylfuran by acetic anhydride. Nevertheless, MgF_2-100 was found to be totally inactive whereas, FeF_3-100 showed a very weak activity, since the yield in 2-acetyl-5-methylfuran measured after 6 h in presence of 500 mg of catalyst at 50 °C was 0.4 mol%. Under the same conditions, the yield into acylated product over AlF_3-100 was close to 20 mol%. These results show that the presence of Brønsted acid sites, at least with sufficient strength, in addition to Lewis acid sites, is required in order to obtain active fluorides in acylation.

3.5. *Proposal of reaction mechanism of acylation of 2-methylfuran by acetic anhydride*

Based on the characterization of the solids and their catalytic results for the acylation of 2-methylfuran by acetic anhydride, some information about the nature of the active sites present on fluoride catalysts can be discussed. Firstly, it was observed that the HY zeolite with a high amount of Brønsted acid sites and a low amount of Lewis acid sites (Table 1, entry 9) exhibited a poor activity in acylation compared to that observed for aluminum hydroxide fluorides, which had significant Lewis acid sites (Table 1, entries 1 to 4). Secondly, a decrease of the amount of Brønsted acid sites in aluminum fluoride catalysts while at the same time maintaining the amount of Lewis acid sites (between 381 and 464 $\mu mol\,g^{-1}$) led to a decrease of the activity in acylation. Thirdly, other fluorides, such as MgF_2 and FeF_3 were found to be inactive for such a reaction, probably imputed to their very weak Brønsted acidity. From these experimental results, the nature of the site involved in the studied reaction could be a Lewis acid site (unsaturated aluminum) in the vicinity of a Brønsted acid site, as already proposed by Coman et al. [37].

The proposed mechanism for the acylation of 2-methylfuran by acetic anhydride is reported in Scheme 2. First of all, acetic anhydride could be activated by its adsorption on unsaturated aluminum, which is the proposed Lewis acid site. The second step could be the formation of an acylium ion involving a neighbor OH which acts as a Brønsted acid site, and thus, the liberation of acetic acid as by-product. The physisorption of 2-methylfuran on the Lewis acid site by its oxygen atom followed by the transfer of the acylium ion can yield an intermediate cation (Wheland complex) depicted in Scheme 2. The attack of acylium ion occurs only in position 2 (on alpha position on the oxygen atom) due to a greater stability of this Wheland complex, as already observed for such furanic compounds [10,11,14]. The last step is desorption of the required product (2-acetyl-5-methylfurane) and the regeneration of the active site.

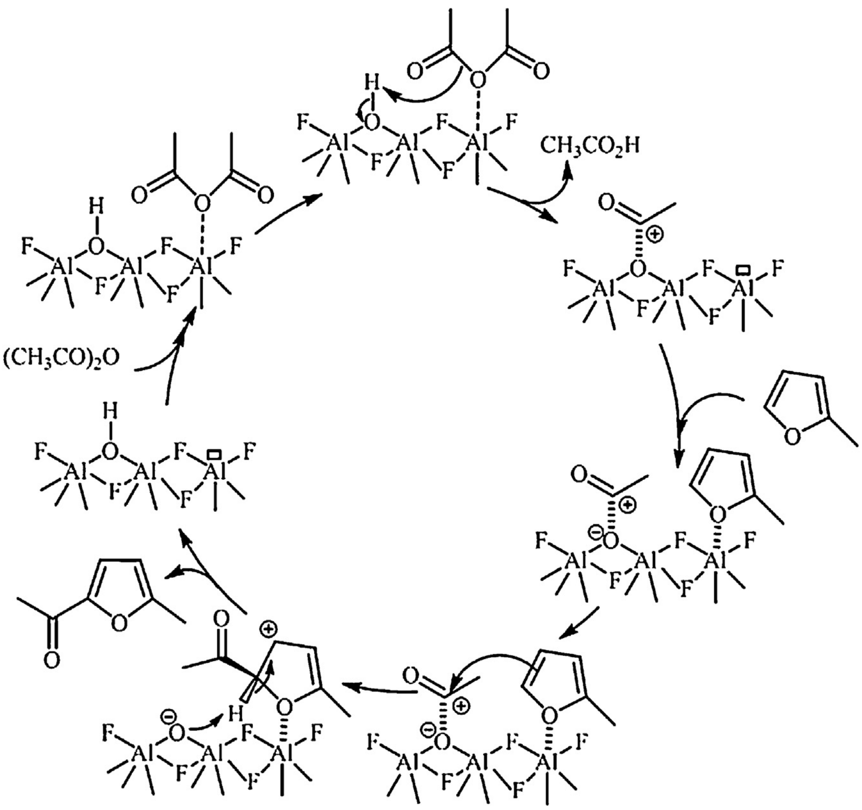

Scheme 2. Mechanism of the acylation of 2-methylfuran by acetic anhydride involving a schematic bi-acid site of aluminum hydroxide fluoride.

4. Conclusions

A heterogeneous catalytic process involving inorganic aluminum hydroxide fluorides ($AlF_{3-x}(OH)_x$) as catalysts was successfully applied for the selective synthesis of 2-acetyl-5-methylfuran from acylation of 2-methylfuran by acetic anhydride. This reaction was performed under mild conditions (50 °C, P_{atm}) and with stoichiometric amount of each reactant, *i.e.*, a solvent-free reaction, this promising process being hence environmentally friendly.

Nanoscopic inorganic aluminum hydroxide fluorides employed as acylation catalysts were found to be the most efficient catalyst among different inorganic fluorides studied in this work (AlF_3, MgF_2, and FeF_3). From different synthesis parameters (calcination temperature, HF/Al ratio), the Lewis/Brønsted ratio of $AlF_{3-x}(OH)_x$ has been tuned, and this interesting flexibility of such a ratio allowed the discrimination of the involved sites for the studied reaction. The high activity in combination with the selectivity into 2-acetyl-5-methylfuran was attributed to the synergistic effect of both Brønsted and Lewis which could be neighboring sites on the surface of the nanoscopic hydroxylated aluminum fluorides. Therefore, their activity was better than a zeolite HY, since the active sites of the latter was clearly different (important Brønsted acidity, but low amount of Lewis acidity).

This work clearly confirms the potential of these nanosized inorganic hydroxide fluorides, which have tunable acid properties, as heterogeneous catalysts for several reactions which need such a combination of active sites, allowing to expand the range of opportunities for such fluoride catalysts.

Acknowledgements

The authors wish to thank Stéphane Pronier for the TEM characterization.

References

[1] E.I. Gürbüz, J.M.R. Gallo, D.M. Alonso, S.G. Wettstein, W.Y. Lim, J.A. Dumesic, Angew. Chem. Int. Ed. 52 (2013) 1270–1274.
[2] S. Dutta, S. De, B. Saha, M.I. Alam, Catal. Sci. Technol. 2 (2012) 2025–2036.
[3] M.J. Climent, A. Corma, S. Iborra, Green Chem. 16 (2014) 516–547.
[4] I. Delidovich, K. Leonhard, R. Palkovits, Energy Environ. Sci. 7 (2014) 2803–2830.
[5] T. Mizugaki, T. Yamakawa, Y. Nagatsu, Z. Maeno, T. Mitsudome, K. Jitsukawa, K. Kaneda, ACS Sustain. Chem. Eng. 2 (2014) 2243–2247.
[6] S. Sitthisa, W. An, D.E. Resasco, J. Catal. 284 (2011) 90–101.
[7] G. Sartori, R. Maggi, Chem. Rev. 111 (2011) PR181–PR214.
[8] G.A. Olah, Friedel–Crafts Chemistry, Wiley, 1973.
[9] R.A. Sheldon, R.S. Downing, Appl. Catal. Gen. 189 (1999) 163–183.
[10] V.F.D. Álvaro, A.F. Brigas, E.G. Derouane, J.P. Lourenço, B.S. Santos, J. Mol. Catal. Chem. 305 (2009) 100–103.
[11] P.R. Reddy, M. Subrahmanyam, S.J. Kulkarni, Catal. Lett. 54 (1998) 95–100.
[12] F. Richard, H. Carreyre, G. Pérot, J. Mol. Catal. Chem. 103 (1995) 51–61.
[13] F. Richard, H. Carreyre, G. Pérot, J. Mol. Catal. Chem. 101 (1995) L167–L169.
[14] F. Richard, H. Carreyre, G. Pérot, J. Catal. 159 (1996) 427–434.
[15] D. Rohan, C. Canaff, E. Fromentin, M. Guisnet, J. Catal. 177 (1998) 296–305.
[16] C. Guignard, V. Pédron, F. Richard, R. Jacquot, M. Spagnol, J.M. Coustard, G. Pérot, Appl. Catal. Gen. 234 (2002) 79–90.
[17] T. De Baerdemaeker, B. Yilmaz, U. Müller, M. Feyen, F.-S. Xiao, W. Zhang, T. Tatsumi, H. Gies, X. Bao, D. De Vos, J. Catal. 308 (2013) 73–81.
[18] E. Kemnitz, S. Wuttke, S.M. Coman, Eur. J. Inorg. Chem. 2011 (2011) 4773–4794.
[19] S.B. Troncea, S. Wuttke, E. Kemnitz, S.M. Coman, V.I. Parvulescu, Appl. Catal. B Environ. 107 (2011) 260–267.
[20] S. Wuttke, A. Negoi, N. Gheorghe, V. Kuncser, E. Kemnitz, V. Parvulescu, S.M. Coman, ChemSusChem 5 (2012) 1708–1711.
[21] M. Chen, J.-M. Jin, S.-D. Lin, Y. Li, W.-C. Liu, L. Guo, L. Li, X.-N. Li, J. Fluorine Chem. 150 (2013) 46–52.
[22] I. Agirrezabal-Telleria, Y. Guo, F. Hemmann, P.L. Arias, E. Kemnitz, Catal. Sci. Technol. 4 (2014) 1357–1368.
[23] A. Astruc, C. Cochon, S. Dessources, S. Célérier, S. Brunet, Appl. Catal. Gen. 453 (2013) 20–27.
[24] M. Pietrowski, M. Zieliński, M. Wojciechowska, ChemCatChem 3 (2011) 835–838.
[25] M. Bonarowska, O. Machynskyy, D. Łomot, E. Kemnitz, Z. Karpiński, Catal. Today 235 (2014) 144–151.
[26] A. Negoi, K. Teinz, E. Kemnitz, S. Wuttke, V.I. Parvulescu, S.M. Coman, Top. Catal. 55 (2012) 680–687.

[27] F. Richard, S. Célérier, M. Vilette, J.-D. Comparot, V. Montouillout, Appl. Catal. B Environ. 152–153 (2014) 241–249.
[28] E. Kemnitz, U. Groß, S. Rüdiger, C.S. Shekar, Angew. Chem. Int. Ed. 42 (2003) 4251–4254.
[29] K. Teinz, S. Wuttke, F. Börno, J. Eicher, E. Kemnitz, J. Catal. 282 (2011) 175–182.
[30] Y. Guo, P. Gaczyński, K.-D. Becker, E. Kemnitz, ChemCatChem 5 (2013) 2223–2233.
[31] G. Scholz, C. Stosiek, M. Feist, E. Kemnitz, Eur. J. Inorg. Chem. 2012 (2012) 2337–2340.
[32] S. Rudiger, U. Grob, E. Kemnitz, J. Fluor. Chem. 128 (2007) 353–368.
[33] Y. Guo, S. Wuttke, A. Vimont, M. Daturi, J.-C. Lavalley, K. Teinz, E. Kemnitz, J. Mater. Chem. 22 (2012) 14587–14593.
[34] S.M. Coman, V.I. Parvulescu, S. Wuttke, E. Kemnitz, ChemCatChem 2 (2010) 92–97.
[35] N. Candu, S. Wuttke, E. Kemnitz, S.M. Coman, V.I. Parvulescu, Appl. Catal. Gen. 391 (2011) 169–174.
[36] C. Dobrinescu, E.E. Iorgulescu, C. Mihailciuc, D. Macovei, S. Wuttke, E. Kemnitz, V.I. Parvulescu, S.M. Coman, Adv. Synth. Catal. 354 (2012) 1301–1306.
[37] S.M. Coman, S. Wuttke, A. Vimont, M. Daturi, E. Kemnitz, Adv. Synth. Catal. 350 (2008) 2517–2524.
[38] S. Wuttke, A. Vimont, J.-C. Lavalley, M. Daturi, E. Kemnitz, J. Phys. Chem. C 114 (2010) 5113–5120.
[39] M. Guisnet, P. Ayrault, J. Datka, Pol. J. Chem. 71 (1997) 1455–1461.
[40] S. Wuttke, S.M. Coman, J. Kröhnert, F.C. Jentoft, E. Kemnitz, Catal. Today 152 (2010) 2–10.
[41] V.M. Meier, D.H. Olson, C. Baerlocher, Zeolites 17 (1996) 104–105.
[42] C. Stosiek, G. Scholz, G. Eltanany, R. Bertram, E. Kemnitz, Chem. Mater. 20 (2008) 5687–5697.
[43] D. Dambournet, A. Demourgues, C. Martineau, E. Durand, J. Majimel, A. Vimont, H. Leclerc, J.-C. Lavalley, M. Daturi, C. Legein, J.-Y. Buzaré, F. Fayon, A. Tressaud, J. Mater. Chem. 18 (2008) 2483–2492.
[44] A. Travert, A. Vimont, A. Sahibed-Dine, M. Daturi, J.-C. Lavalley, Appl. Catal. Gen. 307 (2006) 98–107.